Title: Single cell RNA-sequencing reveals no evidence for meiotic sex chromosome inactivation in the threespine stickleback fish

Daniel E. Shaw, Wynter D. Ross, Alexis V. Lambert, and Michael A. White*

Department of Genetics, University of Georgia, Athens, GA, 30602

Corresponding Author:

Michael A. White

Department of Genetics, University of Georgia

120 Green St,

Athens, GA 30602

whitem@uga.edu

Abstract

Sex chromosomes often evolve unique patterns of gene expression in spermatogenesis. In many species, sex-linked genes are downregulated during meiosis in response to asynapsis of the heterogametic sex chromosome pair (meiotic sex chromosome inactivation; MSCI). Our understanding of this process has been limited to a handful of species, including mammals, *Drosophila*, and *C. elegans.* Based on findings from these taxa, MSCI has been viewed as likely a conserved process. However, in other groups like teleost fish, our understanding of this process is limited. Teleost fish are a noteworthy group to investigate because sex chromosomes can rapidly evolve between closely related species. Transcriptional profiling of spermatogenesis at the single-cell level is a useful approach to investigate whether MSCI occurs in other species with independently derived sex chromosomes. Here, we investigate whether MSCI occurs in the threespine stickleback fish (*Gasterosteus aculeatus*), which have an X and Y chromosome that evolved less than 26 million years ago. Using single-cell RNA-seq, we found that the X and Y chromosomes do not have a signature of MSCI, maintaining gene expression across meiosis. Using immunofluorescence, we also show the threespine stickleback do not form a condensed sex body around the X and Y, a conserved feature of MSCI in many species. We did not see patterns of gene content evolution documented in other species with MSCI. Y-linked ampliconic gene families were expressed across multiple stages of spermatogenesis, rather than being restricted to post-meiotic stages, like in mammals. Our work shows MSCI does not occur in the threespine stickleback fish and has not shaped the evolution of the Y chromosome. In addition, the absence of MSCI in the threespine stickleback suggests this process may not be a conserved feature of teleost fish and argues for additional investigation in other species.

Author Summary

As male germ cells enter meiosis, the X and Y chromosome of many species undergo a drastic repression of gene expression. In mammals, this process has been shown to be essential for fertility, and the expression of sex-linked genes can lead to meiotic arrest and cell death. This process has only been studied in a handful of organisms, which limits our understanding how conserved MSCI is across the tree of life. Teleost fish are an understudied group with many examples of independently derived sex chromosomes across closely related species. Here, we investigate whether MSCI occurs in the threespine stickleback fish, using single-cell transcriptional profiling. We found gene expression remains active throughout meiosis on the sex chromosomes, indicating MSCI does not occur. This indicates that MSCI is not a conserved feature of all taxa and is not an inevitable outcome of degenerating Y chromosomes.

Introduction

Heteromorphic sex chromosomes often fail to fully synapse during meiosis due to a lack of sequence homology between the chromosome pair (i.e. X and Y or Z and W). In mammals, the X and Y chromosomes only synapse within the pseudoautosomal region, where all crossing over is restricted in males (1). Outside of the pseudoautosomal region, the unsynapsed chromatin triggers a process of complete transcriptional silencing and sequestration into a dense sex body, known as meiotic sex chromosome inactivation (MSCI) (2-4). Most genes remain silenced throughout post-meiotic stages (5, 6). MSCI may actually represent a more generalized process of silencing of any unsynapsed chromosomes in male or female meiosis (MSUC; meiotic silencing of unsynapsed chromatin) (7, 8). Although the function of silencing remains unknown,

68 it may have a role in ensuring DNA double strand breaks are properly repaired during meiosis at
69 locations where chromosomes fail to synapse properly (reviewed in (3).
70 MSCI appears to have evolved independently in multiple lineages. In mammals, MSCI
71 evolved in the common ancestor of therians, approximately 180 million years ago after the origin
72 of the X and Y chromosomes (9). Since their origin, the sex chromosomes have diverged
73 structurally in both marsupial and eutherian lineages, yet they still share many meiotic silencing
74 factors that initiate in response to the unpaired X and Y (10, 11). Sex chromosomes
75 independently evolved within monotremes, and while a canonical sex body does not form (12),
76 gene expression is reduced drastically in the non-recombining region in platypus (13), indicating
77 a general mechanism for silencing unpaired chromosomes may have been present in the common
78 ancestor of all mammals. Outside of mammals, sex chromosome silencing occurs across the
79 hemizygous X chromosomes of *Caenorhabditis* species (14) and grasshoppers (15, 16), both of
80 which have XO males, where the X lacks a pairing partner. Some evidence exists for transcript
81 repression from the X chromosome in the XY male germline of *Drosophila melanogaster* (17-
82 20), suggesting MSCI may also exist in this species (but also see (21, 22)).
83 MSCI imposes a strong selection pressure on the overall gene content of evolving sex
84 chromosomes. The X chromosome is a disfavored environment for genes with functions in
85 spermatogenesis if the X is transcriptionally silenced during meiosis (3). One way to circumvent
86 silencing is to move genes from the suppressed sex chromosomes to the autosomes.
87 Retrotransposition of genes has been a major driver of gene content evolution on the mammalian
88 and *Drosophila* X chromosomes (23-25). Another mechanism to circumvent transcriptional
89 suppression during meiosis may be to increase copy number of genes on the X chromosome to
90 produce more RNA transcript in spite of the repressive chromatin environment (3). Many multi-

91 copy gene families on the mouse X chromosome are reactivated post-meiotically despite
92 chromosome-wide transcriptional silencing (26, 27). Large multi-copy gene families also exist
93 on the mouse and bull Y chromosomes that have testis-specific gene expression and have roles in
94 spermatogenesis (28, 29). Sex chromosomes have evolved repeatedly throughout the tree of life,
95 but outside of a few well-characterized species with relatively ancient sex chromosomes it
96 remains unclear the overall extent to which MSCI occurs and whether it is a common selection
97 pressure on sex-linked gene evolution.

98 The degree of synapsis between sex chromosomes can even vary in species where
99 substantial degeneration has occurred on the Y or W chromosomes. Birds have a ZW sex
100 chromosome system that evolved independently from mammals over 120 million years ago (30).
101 Similar to the mammalian Y chromosome, many species of bird W chromosomes share little
102 sequence homology with the Z chromosome (30). Despite this, MSCI does not occur on the ZW
103 sex chromosomes (31). In chickens, the heterologous Z and W chromosomes show complete
104 synapsis in a majority of pachytene oocytes. Incomplete MSCI has also been shown within
105 mammals, where self-synapsis of the X chromosome in some spermatocytes blocks
106 transcriptional suppression of the chromosome (32). Sex chromosomes with little sequence
107 divergence may also synapse more readily during meiosis, preventing MSCI. At the most
108 extreme, sex chromosomes that only differ at a small sex determination region may not interfere
109 with synapsis at all. For example, there is little sequence divergence between the X and Y
110 chromosome in the guppy (33-35), *Poecilia reticulata*, and these chromosomes fully pair with
111 each other during meiosis (36). Additional focus on how different sex chromosomes achieve
112 pairing during meiosis is necessary to understand the extent of MSCI across convergently
113 evolving sex chromosomes.

The threespine stickleback fish *(Gasterosteus aculeatus)* is an excellent species to explore whether MSCI occurs on a degenerating sex chromosome that fully synapses. The threespine stickleback has an X and Y sex chromosome that evolved less than 26 million years ago (37). Since this time, the Y chromosome has diverged from the X chromosome at both the sequence and structural level. The X and Y chromosomes have a 2.5 Mb pseudoautosomal region, where all crossing over is restricted during meiosis (38). The non-crossover region on the Y chromosome has lost nearly half of the ancestral gene content (37, 39). In addition, three pericentric inversions have altered synteny between the X and Y (37, 40). Despite this degeneration, the sex chromosomes fully pair in a non-homologous fashion along their entire chromosomal length during prophase I of meiosis (41). Due to this pairing, we hypothesized that MSCI would not occur during spermatogenesis and consequently this process has not shaped the evolution of gene content on these chromosomes.

In this study, we used single-cell RNA sequencing to characterize sex-linked gene expression throughout spermatogenesis. Consistent with full pairing and synapsis, we did not find a stage-specific down regulation of X- or Y-linked genes across spermatogenesis. The sex chromosomes were also not sequestered into a sex body. Our study indicates asynapsis and MSCI is not an inevitable outcome for all degenerating sex chromosomes and argues for additional research into other sex chromosome systems to understand why some heteromorphic sex chromosomes can maintain synapsis despite a lack of sequence homology.

Results

Identification of stickleback spermatogenic stages using single-cell RNA sequencing

136 The testis is a highly heterogeneous organ and gene expression varies both spatially
137 across cell types as well as temporally across developmental stages (13, 42). Spermatogenesis
138 occurs synchronously in the threespine stickleback (43). At a given developmental stage, the
139 testes will be enriched for premeiotic, meiotic, or post-meiotic cells, along with somatic support
140 cells. In reproductively mature adult males, the testes will mostly contain mature sperm and
141 somatic cells. In order to capture all stages of spermatogenesis, we sequenced testes from lab-
142 reared males at different developmental stages. We sequenced 6147 cells from a single testis
143 dissected from an earlier stage of spermatogenesis and 2652 cells from a single testis dissected
144 from a male at a later stage of spermatogenesis. In order to maximize the total number of stages
145 of spermatogenesis, we also pooled the testes from two additional males from an intermediate
146 developmental stage (6027 cells total). Each had a similar number of gene counts detected
147 (Supplemental Figure 1). Each testis sample cannot be treated as a direct replicate of one another
148 due to the differences in timing of synchronized spermatogenesis. However, we did find many
149 replicated clusters, indicating overlap in stages of spermatogenesis between the testis samples
150 (Supplemental Figure 2). Among the three samples, there was only one unique cell cluster.
151 Because this cluster was only present in a single sample, we removed these cells (cluster 5 from
152 sample 3) from all downstream analyses. Non-replicated clusters could be due to rare cell
153 populations only identified in one sample or derived from batch differences between sequencing
154 libraries (44).
155 To capture all stages of spermatogenesis in a single analysis, we merged the three
156 samples together and scaled gene expression accordingly. Between all of the samples, we
157 recovered a total of 12,136 cells after filtering. Clustering analysis revealed 14 distinct cell
158 clusters (Figure 1). We identified 3,694 differentially expressed genes across all cell clusters

159 (Mann-Whitney U Test). Genes were considered differentially expressed within a cluster if the
160 gene was expressed in 25% of cells within the cluster, had a $\log_2$ fold change > 0.25 for
161 expression compared to all other clusters, and had a significantly different level of expression
162 evaluated with a P-value < 0.01 after correcting for multiple comparisons. Among the
163 differentially expressed genes, we identified those unique to cell-types in order to assign
164 spermatogenesis stages to each cluster. Cell-type specific markers were identified from
165 conserved genes expressed during spermatogenesis across animals, including insects (45, 46),
166 mammals (13, 42, 47-50), and other teleost fish (51-54). Using these markers, we identified most
167 stages of spermatogenesis including spermatogonia, spermatocytes, and spermatids. We also
168 identified multiple clusters of somatic cells. One class of somatic cells clustered separately from
169 spermatogenesis clusters and had differentially expressed genes that were not specific to testis
170 (i.e. hbae5; Cluster 12; Figure 1); mostly genes involved in immune function and blood cells,
171 that likely represent general somatic cells not unique to testis. A second cluster mapped distinctly
172 from spermatogenesis cells and contained similar immune gene expression, but also had some
173 shared expressed genes with the spermatogenesis clusters likely consistent with testis specific
174 somatic cells (i.e. Sertoli, Leydig etc; Cluster 13; Figure 1). For all further analyses, we
175 combined clusters into four major cell type groups to explore differences across major cell types:
176 pre-meiotic, post-meiotic, meiotic, and somatic cells (Figure 1B). Within each of these broader
177 categories, we found that gene expression levels were highly correlated across each testis sample
178 (Spearman Rank Correlation R > 0.65 for all comparisons) (Supplemental Figure 3).
179
180 **Sex-linked genes do not undergo meiotic silencing**

181 In mammals, genes within the non-recombining region of the sex chromosomes are not
182 transcribed (MSCI) (2, 3, 8). To determine whether meiotic silencing has also evolved in
183 threespine stickleback fish, we compared rates of transcription between sex-linked and
184 autosomal genes. We found that gene expression was not reduced on the X chromosome in
185 meiotic cells, relative to somatic and pre-meiotic cell types (Figure 2; $P > 0.05$). While the Y
186 chromosome showed lower expression than the X chromosome, Y-linked genes maintain similar
187 levels of expression across pre-meiotic and meiotic cells (Figure 2, $P > 0.05$). We also examined
188 whether there were unique expression patterns among the differently aged evolutionary strata
189 (Peichel et al. 2020). We found no evidence of silencing among the different regions of the sex
190 chromosomes (Supplemental Figure 4), indicating this is not a phenomenon restricted to even the
191 oldest stratum of the X and Y (stratum 1). Overall, we found that unlike mammals, chromosome-
192 wide silencing does not occur on the threespine stickleback sex chromosomes during meiosis.
193

194 **The threespine stickleback X and Y chromosomes are not condensed into a sex body**

195 During MSCI, the mammalian X and Y chromosomes are sequestered into a dense
196 structure, known as the sex body (2-4, 8). Key markers of this structure are the phosphorylated
197 histone variant, γH2AX (2, 3, 6, 55) and H3K9me3 (55). In the threespine stickleback, the X and
198 Y chromosome likely synapse fully and do not show evidence of delayed DSB repair (41).
199 Together with our results that gene expression was not suppressed throughout meiosis, we
200 predicted that a mammalian-like MSCI sex body would also not be present during
201 spermatogenesis. To test this, we characterized how γH2AX accumulated throughout meiosis
202 using immunofluorescence. γH2AX broadly localized to all chromosomes beginning at leptotene
203 in response to the initiation of DNA double strand breaks (56) (Figure 3). During pachytene,

204 double strand breaks are repaired and we observed a reduction of γH2AX foci, similar to patterns
205 observed in mammals (2). However, we did not observe an aggregation of γH2AX synonymous
206 with a sex body in late meiosis. We staged a total 146 nuclei from leptotene to pachytene. None
207 of the scored nuclei had any structure resembling a sex body. This result is consistent with the
208 expression data supporting that canonical MSCI does not occur in threespine stickleback fish due
209 to the lack of asynapsis and sex body formation.
210
211 **Gene evolution on the sex chromosomes has not been shaped by MSCI**
212 In addition to the ancestral complement of gametologs shared between the X and Y, the
213 Y chromosome has also acquired unique genes that originated from the autosomes (37). After
214 translocation to the Y chromosome, many of these genes have further duplicated and evolved
215 testis-biased expression, suggesting a gain of spermatogenesis function (37). In mammals, the
216 ancient Y chromosome has also accumulated species-specific gene duplicates that are enriched
217 for post-meiotic expression and have been speculated to be involved in intra-genomic conflicts
218 between X and Y bearing sperm during spermatogenesis (26, 28, 29, 57-60). Due to the absence
219 of meiotic silencing in stickleback fish, we characterized how the expression of these Y-linked
220 duplicates compared to mammalian amplicons. We looked at the overall expression of all
221 paralogous copies within each gene family and assayed whether there were differences across the
222 four major cell types of spermatogenesis. We found that the Y-linked duplicated genes were
223 expressed across multiple cell types of spermatogenesis (Figure 4). Interestingly, in the absence
224 of chromosome wide silencing in meiosis, we found the highest number of expressed duplicate
225 families (104) in meiotic cell types, and expression for many duplicate families is highest in
226 meiosis compared to all other cell types (Figure 4). This was true for many genes, regardless of

227 the total number of paralogs, which ranged from 2-30 copies. This suggests that many amplicons
228 on the threespine stickleback Y chromosome may have functions throughout meiosis, rather than
229 post-meiotic stages as has been observed in mammals.

230 We searched for an enrichment of GO terms among the expressed duplicate genes to
231 assign function. We found that the predominant functions included chromatin assembly, DNA
232 packaging, and DNA repair. Specifically, we found many expressed duplicate families were
233 genes with critical functions in meiosis, including proteins involved in double strand break repair
234 (RAD proteins) and proteins involved in chromosome synapsis and segregation (SMC proteins)
235 (61). Together, these results provide novel insight into the functions of duplicated Y-linked
236 genes, which in other species have been associated with post-meiotic expression (57, 58, 62).
237 Specifically, this finding highlights the role of meiotic functions in duplicated gene families
238 expressed on the Y, in the absence of meiotic silencing.

239 We searched for evidence of retrotransposition of genes throughout the genome, which
240 occurs at an increased frequency from the X chromosome in species with MSCI (23, 63-65).
241 Unlike these species, we did not find an excess of retrotransposition from the X chromosome in
242 the threespine stickleback. We identified nine examples of retrotransposition since the threespine
243 stickleback shared a common ancestor with the ninespine stickleback *(Pungitius pungitius)*
244 approximately 26 million years ago (66-68) (Supplemental Table 1). None of the nine
245 retrotransposition events originated from the X chromosome. Even though the threespine
246 stickleback Y chromosome shares many features of gene content evolution that have been
247 observed on the mammalian Y chromosome (37, 39), our results highlight that MSCI has not
248 been a driving force shaping these patterns.
249

250 **Genes have similar signatures of selection across stages of spermatogenesis**

251 In other species, different stages of spermatogenesis have opposing signatures of
252 selection (13, 69-71). In house mice for example, cell types in early stages are more
253 evolutionarily constrained, while later stages show signatures of rapid evolution, and this pattern
254 is more extreme on the X chromosome (70). Because we do not observe meiotic silencing in
255 threespine stickleback, we hypothesized we would not find similar differences in signatures of
256 selection across stages of spermatogenesis. We compared non-synonymous and synonymous
257 substitutions rates within genes induced within each of the four identified cell-type groups. We
258 found that dN/dS of autosome genes was similar across spermatogenesis, with the exception of
259 post-meiotic clusters which contained an excess of genes with elevated dN/dS (Figure 5, P =
260 0.006, Kruskal-Wallis and Dunn's test). Consistent with a lack of sex chromosome silencing, we
261 did not observe any differences in dN/dS on the X chromosome across stages of spermatogenesis
262 (Figure 5, P = 0.862, Kruskal-Wallis and Dunn's test).

263

264 **Discussion**

265 The repression of sex chromosomes during meiosis was first noted based on early
266 cytological evidence that many sex chromosomes were found in a condensed chromatin state
267 (72-75). Condensation of the X chromosome was proposed to be a critical feature of
268 spermatogenesis, and could result in sterility if disrupted (72). Since then, several hypotheses
269 have been generated to explain the importance of why sex chromosomes are condensed and
270 silenced including: to help avoid ectopic recombination, facilitate DSB repair, silence genes with
271 deleterious DNA damage, or act as a meiotic checkpoint response (3, 73). Molecular studies
272 have revealed that MSCI, in mouse, is initiated by the unsynaped state of the X and Y in male

273 meiosis during the pachytene stage and results in a complete lack of protein coding expression
274 (2, 8).
275 In this study, we found that the threespine stickleback X and Y chromosome maintain
276 relative expression of genes across all stages of spermatogenesis. Our findings align with
277 previous observations that the X and Y chromosomes fully pair during meiosis (41). If the sex
278 chromosomes are fully associating in a non-homologous fashion, this would prevent MSCI from
279 occurring. In other species with heteromorphic sex chromosomes, full pairing has been shown to
280 occur despite an overall lack of homology between the chromosomes. Each documented case
281 thus far has revealed different mechanisms to achieve this. In the platypus, for instance, cohesins
282 (SMC3) differentially accumulate on the five X and five Y chromosomes during meiosis (76).
283 Although the exact function of the increased recruitment of cohesins to the sex chromosome
284 axial cores remains unknown (12, 76). The threespine stickleback sex chromosomes do not
285 exhibit differential accumulation of SMC3 between the sex chromosomes and autosomes (41),
286 suggesting this is not required in all species for non-homologous pairing. In the chicken, the Z
287 chromosome undergoes synaptic adjustment to pair with the W (77). This is followed by
288 assembly of the central element of the synaptonemal complex, indicating full synapsis of non-
289 homologous regions of the chromosomes (31, 78). Consequently, MSCI does not occur (31).
290 Synaptic adjustment of the longer sex chromosome is also observed during pairing in the
291 threespine stickleback fish (41). However, it remains unknown if full synapsis is also achieved
292 between the X and Y (41). Both the X and Y chromosomes appear closely associated and
293 synapsed during prophase I of meiosis based on localization of the axial element, SMC3, but
294 without higher resolution microscopy, it cannot be ruled out that some regions are not fully
295 synapsed (41). Additional work is necessary to understand if central element components, like

296 SYCP1, are also recruited during non-homologous pairing of the threespine stickleback X and Y
297 chromosomes and if full synapsis is required to prevent MSCI from occurring.
298 Alternatively, it is possible MSCI is not a conserved feature of all taxa and it does not
299 occur in stickleback fish. The initial finding that MSUC occurred in taxa as diverse as
300 *Neurospera crassa, C. elegans*, and mammals lead researchers to believe that MSCI may be
301 initiated in all species with divergent, heteromorphic sex chromosomes (79). However, in
302 chickens the Z and W chromosomes fail to synapse in a subset of oocytes and MSCI is not
303 triggered in these cells (31), indicating MSCI is not necessarily conserved across the tree of life.
304 In teleost fish, the existence of MSUC and MSCI remains unclear and has only been investigated
305 in a few species (80). The swamp guppy *(Micropoecilia picta)* has a degenerated Y chromosome
306 relative to the X chromosome, yet cytological investigations of meiosis revealed no presence of
307 an obvious sex body that would indicate MSCI (81). If MSCI does not occur within teleost fish,
308 the X and Y chromosomes of the threespine stickleback would not need to fully synapse outside
309 of the pseudoautosomal region and MSCI would not be triggered.
310
311 **The Y chromosome does not have signatures of gene content evolution from MSCI**
312 Chromosome-wide silencing creates strong constraints on sex-linked genes and inhibits
313 selfish genetic elements from being expressed in meiosis (82-84). Sex chromosomes are
314 suspected to be an evolutionary hotspot for the accumulation of selfish genetic elements that can
315 bias chromosomal transmission (83-85). As the threespine stickleback sex chromosomes
316 maintain meiotic and post-meiotic expression, we predicted they would not have these signatures
317 of evolution. We found that genes expressed in meiotic and post-meiotic cells on the X
318 chromosome exhibited similar rates of protein coding evolution compared to genes expressed in

319 other cell types. In addition, we did not find an enrichment of retrotransposition of genes of the
320 X chromosome as has been documented in other species with MSCI (23, 63, 64). This suggests
321 that the lack of MSCI and post-meiotic repression of genes has not resulted in the type of gene
322 content evolution that has been linked to genetic conflict.

323 Y chromosomes across many species have been found to accumulate gene duplications of
324 testis specific genes (28, 29, 37, 60, 86, 87). Sex-linked gene amplification has been
325 hypothesized to be the result of selection pressure to escape the repressive environment of
326 silenced chromosomes. Genes escaping post-meiotic repression in mammals have been
327 putatively linked to transmission distortion (26-29, 59, 62, 88). In the absence of MSCI in the
328 threespine stickleback, we observed that Y-linked duplicates were not enriched in post-meiotic
329 stages. Instead, amplified gene families were expressed throughout meiosis. Y-linked gene
330 duplications on the neo-Y chromosome of *Drosophila miranda* were also found to be expressed
331 during meiosis, rather than being restricted to post-meiotic cell types (Wei et al. 2024).
332 Therefore, it may be possible that the enrichment of large ampliconic families during post-
333 meiotic stages may be restricted to mammalian lineages where repression of gene expression
334 extends beyond the meiotic stages of MSCI.

335 To date, no specific genes have been found to cause segregation distortion in threespine
336 stickleback fish, although two microsatellites have been found to have distorted transmission in
337 an F2 cross (89). While most lab crosses yield 50:50 sex ratios, some wild populations have been
338 found to be female biased (90). This could suggest that selection to repress conflicts to maintain
339 even sex ratios is ongoing. Similar to duplicated genes across mammals (28, 59) and *Drosophila*
340 (60, 87, 91), we did find that some gene duplicated gene families duplications on the threespine
341 stickleback Y chromosome were also expressed in post-meiotic stages. Despite the lack of

342 repression in threespine stickleback, we identified several enriched categories of genes similar to
343 other species, including functions in chromatin assembly and maintenance. The well
344 characterized *Segregation Distorter* meiotic drive system in *Drosophila melanogaster*, distorts
345 transmission by manipulating chromatin state of other cells leading to sperm dysfunction and
346 near-complete transmission of the *Sd* locus (92). We also found an enrichment of genes involved
347 in DNA double strand break repair, including elements in the synaptonemal complex, *Smc5.* Y-
348 linked copies of this gene were expressed across both meiotic and post-meiotic stages. Similarly,
349 some of the ampliconic sex-linked gene families in *Mus musculus* (*Slx/Sly*) are orthologs of
350 another synaptonemal complex protein, SYCP3 (93). Deletions and duplications of *Slx* have
351 been found to alter sex ratios in mice (26). While the exact mechanisms of how these genes
352 affect transmission are unknown, the role of recombination proteins being duplicated and neo-
353 functionalized across independently derived Y chromosomes is intriguing. Functional testing of
354 the stickleback sex-linked genes may identify a similar role in transmission distortion.
355 Comparative work across multiple species has showed that several signatures of
356 spermatogenesis have evolved repeatedly, including the amplification of Y-linked
357 spermatogenesis genes, and meiotic/post-meiotic repression. While some features have evolved
358 convergently, many are not conserved across all species (3, 21, 31, 32). The vastly different
359 reproductive strategies and ecological factors affecting fish may alter some of the assumptions
360 made by classic conflict models proposed in mice and flies, and the absence of sex-linked
361 silencing in stickleback fish could be a result of having less selfishness in the male germline.
362 Most segregation distorter genes have been identified in species with internal fertilization like
363 mice and flies (92, 94, 95). Externally fertilized eggs in fish could allow for increased male-male
364 competition (96), which may limit the pervasiveness of genomic conflict, due to the deleterious

365 effects on sperm production associated with selfishness (97). However, reproductive strategies
366 can vary greatly across different species of fish. For example, male stickleback fish court females
367 by building nests, and then provide early stage paternal care by guarding clutches of eggs laid by
368 the female (98), though this behavior does not completely defend against other males (99).
369 Broader comparisons across teleost fish would provide an interesting approach to study these
370 differences in a comparative framework, as there is variation in the types of mating behaviors,
371 reproductive strategies, and sex chromosomes, across closely related species. Specifically, it
372 would be noteworthy to compare the pervasiveness of male-male competition to the rate of
373 selfish evolution in spermatogenesis.
374
375
376 **Methods**
377 **Dissociation of testes for single-cell RNA sequencing**
378 Procedures using threespine stickleback fish were approved by the University of Georgia
379 Animal Care and Use Committee (protocol A2024 08-009-Y1-A0).
380 We performed three runs of single-cell RNA sequencing. Two runs were conducted with
381 a single male fish. The third run was a pool of males (see below). Each male was collected from
382 separate clutches of lab strains derived from wild-caught fish from Port Gardner Bay,
383 Washington. Individuals were selected based on age (~7 months), testis size, and testis
384 coloration, all of which are indicators that male fish are becoming reproductive and
385 spermatogenesis is proceeding. Stickleback fish have synchronous spermatogenesis. We
386 therefore aimed to select one male that was enriched for cells undergoing meiosis and one male
387 that was enriched for post-meiotic cells. The first male had slightly smaller and lighter colored

388 testes, consistent with earlier meiotic stages, while the second had larger, darker testes consistent
389 with later stages of testis maturation. We sequenced a third pool of two males as a replicate of
390 the first two sequencing runs. We identified two males with different testis coloration and size,
391 which were at different stages of spermatogenesis. Both males were seven-month-old fish
392 collected from separate clutches of fish derived from the same Port Gardner Bay population. We
393 pooled one testis from each male together for tissue dissociation and sequencing.

394 Cell dissociation was performed separately for each individual. Both testes from each
395 male were placed in ice cold PBS + 0.04% BSA. We followed a previously published single-cell
396 dissociation method from mice testis (47). We first minced the tissue into small pieces with
397 McPherson-Vannas scissors in 200 µL of digestion medium (1mg/mL DNASE, 1mg/mL
398 collagenase/dispace, 1mg/ML hyaluronidase in solution of DMEM/F12). The cell solution was
399 incubated at 37º C for 10 minutes. The cells were filtered through a 40 µm cell strainer to obtain
400 a single-cell suspension, followed by centrifugation at 4º C, 400g for 10 minutes. The pelleted
401 cells were resuspended in 1mL of cold PBS + 0.04% BSA. Cell viability was assessed using
402 trypan blue. From the staining, we determined approximately 90% of the cells were viable. The
403 cells were immediately processed for sequencing using the 10x genomics single-cell sequencing
404 platform with 3' capture. 10X chromium and subsequent Illumina sequencing were both
405 performed at the Georgia Genome and Bioinformatics Core (University of Georgia).
406

407 **Processing of single-cell RNA-sequencing data**

408 The sequencing reads were demultiplexed with CellRanger (v 4.0.0) mkfastq with
409 bcl2fastq (Illumina) with default parameters. We ran CellRanger mkref on the threespine
410 stickleback genome assembly (v5.0) (37, 100). We aligned fastq reads from all three samples

separately using CellRanger count with default parameters, plus the parameter --chemistry=SC3Pv3. To filter for high quality cells, we used Seurat (v 4.0) to remove cells with > 3000 and <200 unique features (i.e. expressed transcripts) and cells with > 5% mitochondrial counts. Cells with too many or too few identified features likely represent doublets or dead cells, respectively. Transcript expression was normalized using Seurat (v4.0) scaledata, with default parameters. After filtering each dataset separately, we merged all three sequencing runs using Seurat merge, with default parameters. We then performed an analysis on the total dataset, first by identifying cells from each dataset that are contained within nearest neighbors (anchors), by running FindIntegrationAnchors with the dimensions set to dims = 1:20. Then we used Seurat IntegrateData. This step defines a distance between datasets as the total number of cells in the smaller dataset divided by the total number of anchors between each dataset, computes all pairwise distances between each dataset, and clusters the distance matrix to determine a guide tree. After the cells from each dataset were integrated, expression was scaled across each gene, using scaledata. Finally, cells were reassigned to neighbors, clusters, and UMAP was run on the complete dataset.

Clustering and UMAP

We followed the Seurat (v4.0) workflow (101) to perform cell clustering. We determined dimensionality of the dataset by performing a jackstraw permutation in Seurat. Based on the elbow plot and jackstraw plot (Supplemental Figure 5), we identified 20 significant principal components for the integrated dataset with a $P < 0.001$. We ran Seurat findneighbors (Dims:1:12) and Seurat findclusters (Resolution=0.8). Graph-based clustering is performed based on construction of a nearest neighbor graph, and then applies a Leiden community detection

434 algorithm. The resolution factor is recommended to be between 0.4-1.2
435 (https://satijalab.org/seurat/articles/pbmc3k_tutorial.html). We experimented with a range of
436 values from 0.4-1.2 and found that the number of clusters from 0.8 was the most consistent with
437 marker identification and the total number of expected cell types in the threespine stickleback
438 testis (102, 103). To visualize the clusters, we ran the Seurat UMAP function set to 20
439 dimensions (Dims=1:20). We verified that most clusters had a similar number of reads per cell,
440 and expressed features per cell, to avoid identifying clusters based on read depth alone
441 (Supplemental Figure 6).
442
443 **Identification of cell clusters**
444 Differentially expressed genes were identified using the FindAllMarkers function in
445 Seurat. A Mann-Whitney U test was used to compare gene expression of each gene across all
446 clusters to identify significantly different gene expression profiles between clusters. Genes were
447 considered differentially expressed between clusters if there was a p-value < 0.001 after
448 correcting for multiple comparisons based on a Bonferroni correction. To relate cell clusters to
449 known cell types, we identified upregulated genes specific to clusters that were well
450 characterized genes from mammals (42, 45, 47-50) and fish (51, 52). We also identified genes
451 expressed during meiosis that are conserved at the coding sequence across mammals (104, 105).
452
453 **Gene ontology**
454 We used the ShinyGO v0.741 web-based tool to identify gene ontology of upregulated
455 genes for each cluster with the genome set to "Stickleback" and processes set to "All available
456 gene sets." We used all stickleback genes expressed in our single-cell RNA dataset as the

457 background, to identify enrichment of biological processes involved in the significantly up-
458 regulated genes of each cluster. For each set of genes, fold enrichment of percentage of genes
459 within a pathway along with a false discovery rate (FDR). We only retained GO terms with an
460 FDR < 0.01.
461
462 **Gene expression across the sex chromosomes**
463 To analyze chromosome-wide expression patterns across cells within a cluster, we
464 extracted alignments from each cluster output using pysam (v 0.16.0.1) and a custom python
465 script (https://github.com/daniel-shaw1/Single-Cell-RNA-
466 sequencing/blob/main/Split_bam_by_cluster.py), that separates RNA alignments for each
467 cluster. Splitting of alignment files was ran separately for each of the three independent samples
468 based on CellRanger clustering. We counted the total number of reads that aligned within genes
469 for each cluster using htseq-count (v 0.13.5) (-mode union --nonunique all --minaqual 1 –
470 stranded=no) (106). These parameters were previously used to identify expression of Y-linked
471 genes in threespine stickleback with bulk RNA-seq (37). We counted within genes of the Y
472 chromosome (37) as well as predicted genes on the autosomes and X chromosome from Ensembl
473 build 107. Reads were counted across the entire transcript as one feature. To assess how gene
474 expression changes on the X and Y chromosomes relative to autosomes across spermatogenesis,
475 we normalized the total expression of each gene on the X and Y by the median expression of all
476 genes across the autosomes of each cluster and then cluster counts were averaged into four
477 categories for each major stage(i.e. somatic, pre-meiotic, meiotic, or post-meiotic).
478 We also assayed gene expression of duplicate gene families across the Y chromosome
479 that were previously annotated (37). To analyze overall expression level of each duplicate gene

480 family, we counted the total number of reads that aligned to each paralog within the family and
481 then summed these counts across all paralogs to get an overall count for each duplicate gene
482 family. We normalized counts for each duplicate gene family per cluster by dividing by the
483 library size of each cluster. Normalized gene duplicate expression was plotted using Morpheus
484 (https://software.broadinstitute.org/morpheus.)
485
486 **Detection of retrotransposition throughout the genome**
487 We searched for evidence of retrotransposition of genes from the autosomes and the X
488 chromosome. We aligned all protein coding sequences from the threespine stickleback (NCBI
489 release 100) to the threespine stickleback genome assembly (v. 5) (100)**.** In order to identify
490 putative retrotranspositions unique to threespine stickleback lineage after the X and Y
491 chromosomes evolved, we also aligned the threespine stickleback protein coding sequences to an
492 outgroup species, the ninespine stickleback (v. 2.1 genome) (107)**.** We aligned all protein
493 sequences using Exonerate (v. 2.4) with parameters --model protein2genome --cores 8 --bestn 5 -
494 -showalignment FALSE --showvulgar TRUE --ryo "%ps\\n" (108). We searched for protein
495 sequences that had greater than or equal to one intron that aligned to a second location in the
496 threespine genome with zero introns. These putative retrotranspositions were confirmed to be
497 specific to the threespine stickleback by verifying the alignment did not exist on the orthologous
498 chromosome of the ninespine stickleback.
499
500 **Protein coding divergence**
501 In order to compare coding sequence evolution, we aligned the threespine stickleback
502 fish CDS (Ensembl release 107) (109) to the ninespine stickleback genome (68) using Exonerate

503 (v. 2.4) (exonerate --model est2genome -M 2000 --bestn 15 --percent 25) (108). We ran codeml
504 from the PAML (phylogenetic analysis by maximum likelihood) (runmode =-2) software
505 package (110) to calculate d_N, d_S, and d_N/d_S for all alignable coding sequence between the
506 threespine and ninespine stickleback. Exonerate alignments were filtered to remove stop codons
507 and gaps, and processed into a codeml compatible input using a custom Perl script
508 (https://github.com/daniel-shaw1/Single-Cell-RNA-sequencing), modified from a previous study
509 (39). For genes with multiple annotated transcripts that aligned between the threespine and
510 ninespine stickleback, d_N/d_S ratios were averaged across the transcripts. Genes with a d_N/d_S value
511 of 99 were removed as these values are unreliable and occur when a gene does not have
512 synonymous substitutions.
513
514 **Meiotic chromosome spreads**
515 The methods used for chromosome spreads were adapted from a protocol for zebrafish
516 (111). We collected fish that were undergoing meiosis that were five to eight months in age and
517 had minimal pigmentation of the testes (41). Whole testes were removed and submerged in 1 mL
518 of 1X PBS inside a 1 mL Douce homogenizer. The tissue was homogenized by grinding with the
519 tight pestle approximately 10 times. The entire volume of cell suspension was transferred to a 1.6
520 mL tube and centrifuged at 500 xg for five minutes. The supernatant was then removed and the
521 pellet was resuspended in 600 µL of 0.8% sodium citrate. The volume of sodium citrate was
522 adjusted based on the size of the pellet to achieve a low turbidity solution. The sodium citrate,
523 cell suspension was incubated at room temperature for five to eight minutes. 20 µL of the cell
524 suspension and 20 µL of 100mM sucrose was pipetted onto each slide and spread by gently
525 tilting the slide. 100 µL of 1% (pH 8.5, adjusted with 0.1 M sodium tetraborate)

526 paraformaldehyde solution with 0.15% TX-100 was then added and spread across each slide
527 before being incubating in a humid chamber at room temperature for two and a half hours. After
528 incubating the slides, we removed the top of the humid chamber to cure the slides overnight.
529 After curing, the slides were washed 3 consecutive times for 15, five, and five minutes in 1X
530 PBS with gentle agitation. Slides were allowed to dry for 15-20 minutes before
531 immunofluorescence or storing at –20°C.
532
533 **Immunofluorescence staining of SMC3 and γH2AX**
534 1.5 mL of permeabilization solution (1X PBS, 1 mM EDTA, and 1% TritonX-100) was
535 pipetted onto the slides and incubated at 20 minutes at room temperature. After dumping off the
536 solution, the slides were blocked with 1.5 mL of 1X antibody dilution buffer, incubating at room
537 temperature for 30 minutes. A 1:80 dilution of primary antibodies in 40 µL total volume was
538 pipetted on each slide (anti-SMC3, Abcam ab9263; anti- γH2AX, DSHB UNC93-5.2.1). The
539 slides were sealed with coverslips and rubber cement before being incubated in a humid chamber
540 overnight at 4°C. After incubating overnight, the coverslips were allowed to float off in 1X PBS,
541 and the slides were blocked with 1.5 mL 1X antibody dilution buffer for 30 minutes at room
542 temperature. A 1:100 dilution of secondary antibodies in 40 µL total volume was pipetted on
543 each slide (goat anti-rabbit Alexa Fluor 488, Abcam ab150077; goat anti-mouse Alexa 568,
544 ThermoFisher A-21134). The slides were sealed with coverslips and rubber cement before
545 incubating in a humid chamber at 37°C for two to three hours. After the coverslips were
546 removed, the slides were washed three times for 15, five and five minutes in 1X PBS with gentle
547 agitation. 40 µL of Vectashield Antifade Mounting Media with DAPI (Vector Labs) was added
548 to the slides and sealed with coverslips and nail polish.

549

550 **Staging of Meiocytes and Super Resolution Imaging**

551 The chromosome spreads were viewed and staged with a Nikon Eclipse Ti2 Microscope
552 with a 100x oil immersion lens. Prophase I stages were identified with the following criteria:
553 small, non-contiguous stretches of SMC3 were defined as leptotene; long SMC3 pieces and
554 incomplete strands indicating an absence of synapsis were defined as zygotene; and pachytene
555 was identified by fully formed SMC3 strands, suggesting complete synapsis. Final images were
556 taken with a Zeiss Elyra S1 (SR-SIM) Super Resolution Microscope with 100x oil immersion
557 lens. The images were processed with ImageJ and Zeiss Black software.

558

559 **Data availability**

560 The data for this manuscript is available within the short reads archive under accession numbers:
561 XXXXXXXX
562 Scripts and bioinformatic pipelines are available at: https://github.com/daniel-shaw1/Single-
563 Cell-RNA-sequencing
564 All microscopy images are available upon request.

565

566

567 **Acknowledgements**

568 This work was supported by the National Science Foundation MCB 1943283 (M.A.W.), the
569 National Institutes of Health R01GM147312 (M.A.W.), the University of Georgia Research
570 Foundation (D.E.S.), and by the Society for Study of Evolution R.C. Lewontin Early Award

571 (D.E.S). Single cell library preparations and sequencing were performed at the UGA Georgia
572 Genome and Bioinformatics Core.
573

574 **Declaration of interests**

575 The authors declare no conflicts of interests.

576 **Figures**

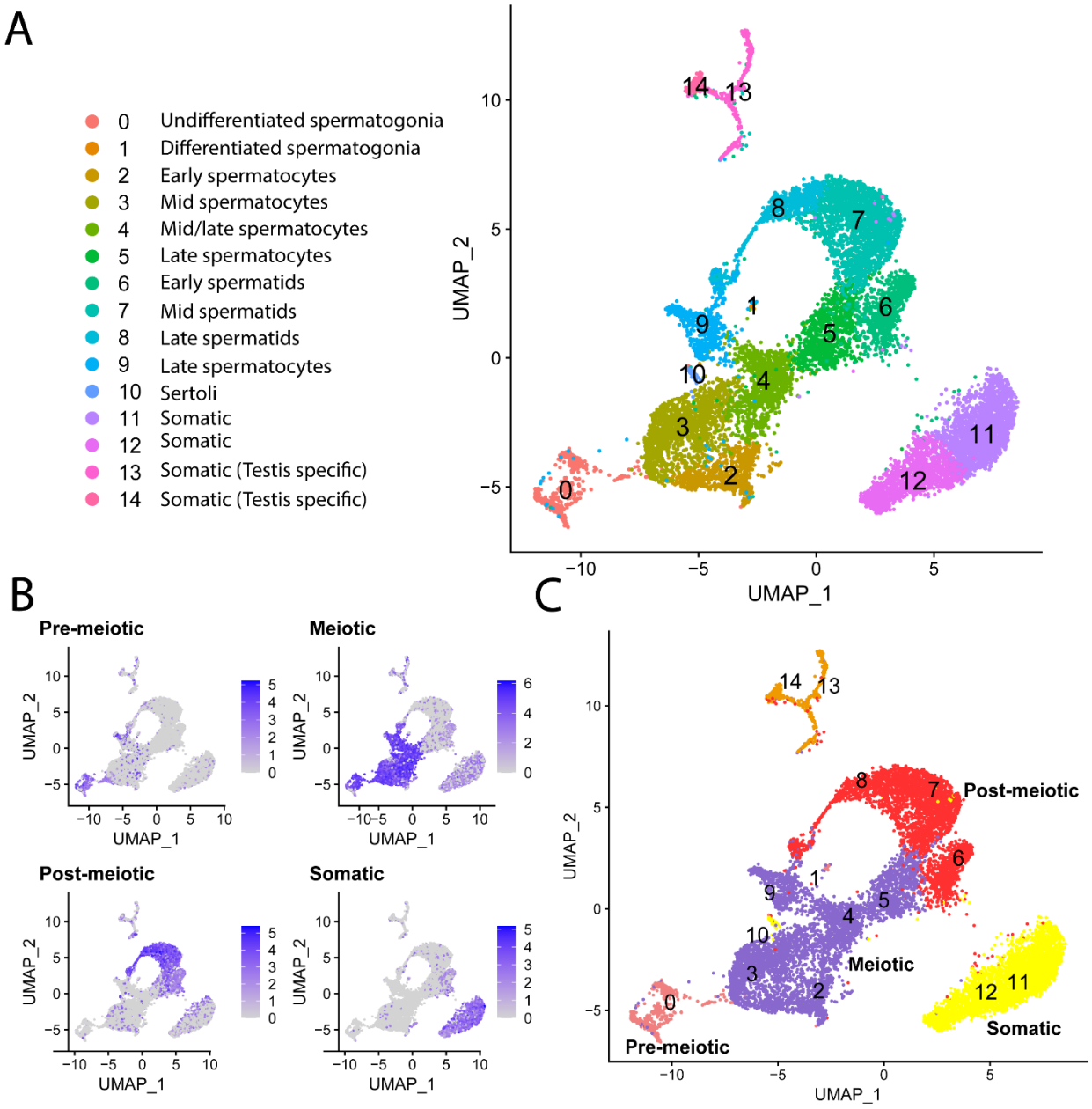

577

578 **Figure 1. Single-cell RNA-seq of threespine stickleback spermatogenesis.** Identified clusters

579 of pre-meiotic, meiotic, post-meiotic, and somatic cell populations integrated from three

580 sequencing runs. (**A**) Visualization of single-cell expression profiles of spermatogenesis in

581 UMAP projection. We identified 15 clusters and related them to stages of spermatogenesis based

582 on significantly upregulated marker genes and GO terms (Table 1). (**B**) Examples of enrichment

583 of key marker genes across the four main stages of spermatogenesis. Additional marker genes

584 are in Table 1. (**C**) The four main spermatogenesis stages overlaid on the UMAP projection.

585

586

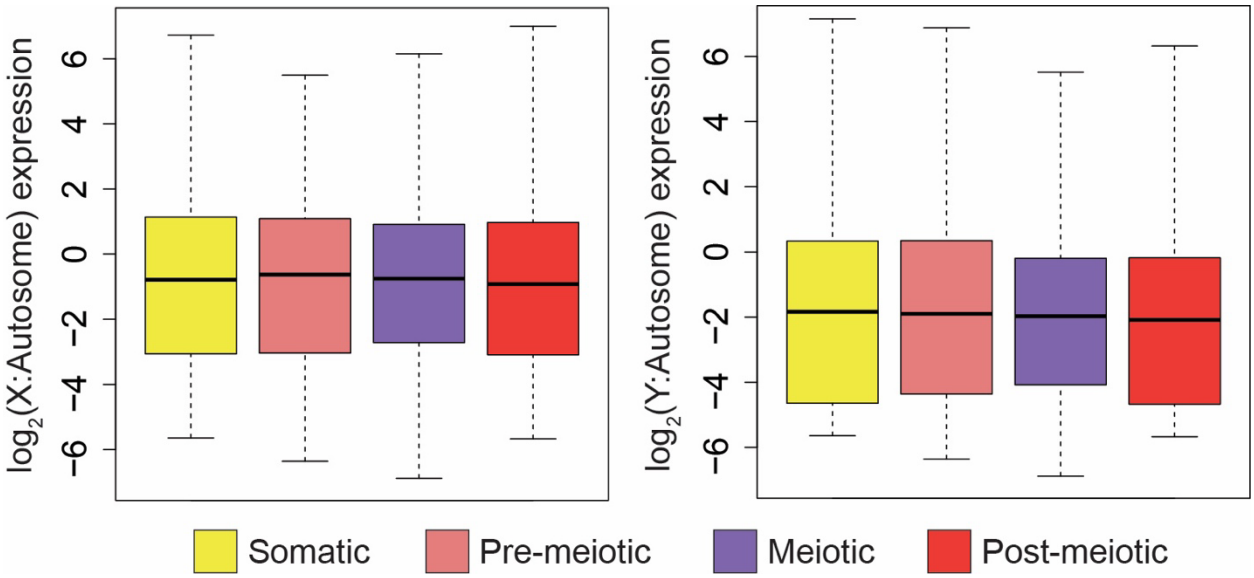

587

588 **Figure 2. Sex-linked gene expression does not change across spermatogenesis**. X- and Y-

589 linked gene expression was normalized to median autosome expression level for each stage of

590 spermatogenesis. Relative to median autosome expression, X- (left) and Y-linked (right) gene

591 expression does not change across stages of spermatogenesis. (Pairwise Mann-Whitney U Test, P

592 > 0.05). Outliers are not shown.

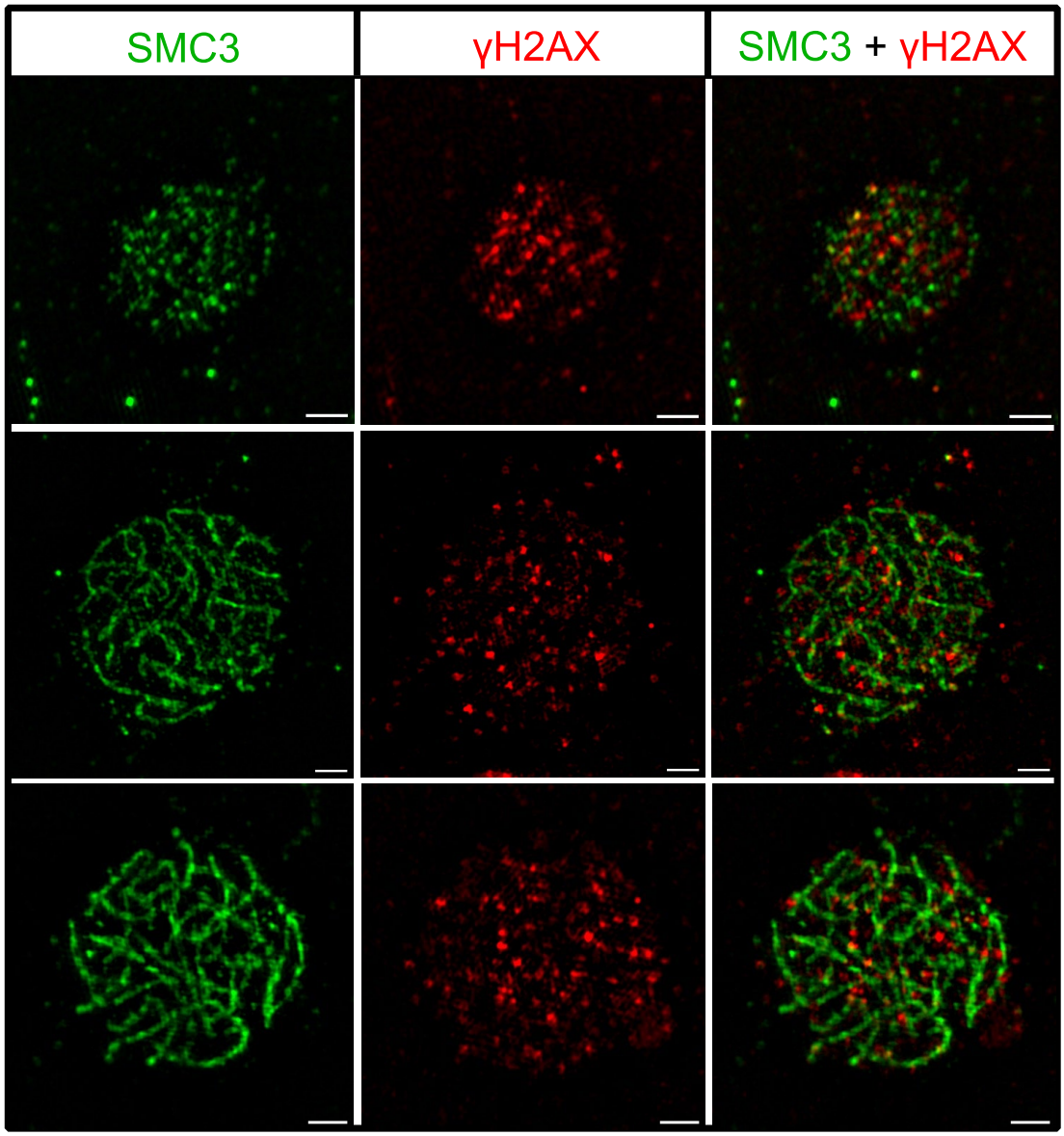

Figure 3. The X and Y chromosomes are not sequestered into a sex body. The highest density of the phosphorylated histone variant, γH2AX, a marker of DNA damage (red) occurs during leptotene (top), when the greatest number of DNA double strand breaks also occur. γH2AX localization decreases as double strand breaks are repaired in zygotene (middle) and pachytene (bottom). The sex chromosomes are repaired at the same rate since they are not

599 sequestered into a dense, γH2AX containing sex body at pachytene. The synaptonemal complex

600 axes are immunolabeled against the axial protein, SMC3 (green). The scale bar is 5 µm.

601

602

603

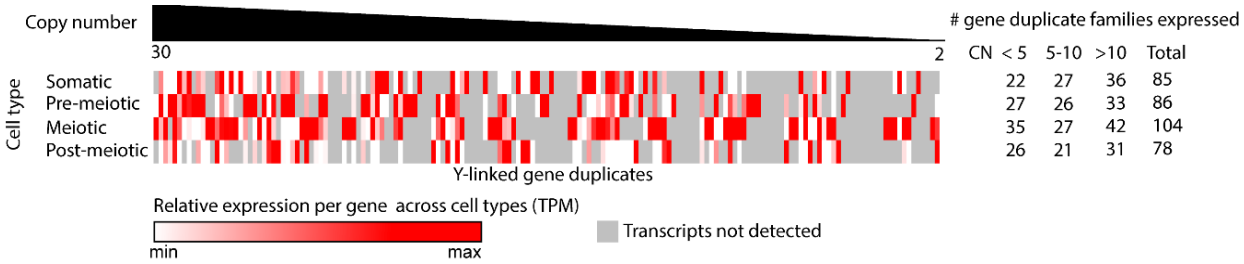

604

605 **Figure 4. Y-linked duplicate gene families are expressed across stages of spermatogenesis.**

606 Duplicate gene families on the Y chromosome assembly are enriched for expression during

607 spermatogenesis. The greatest number of duplicate families were found to be expressed in

608 meiotic cell types. Normalized counts for all paralogous copies of a gene family were summed to

609 determine an aggregate expression level.

610

611

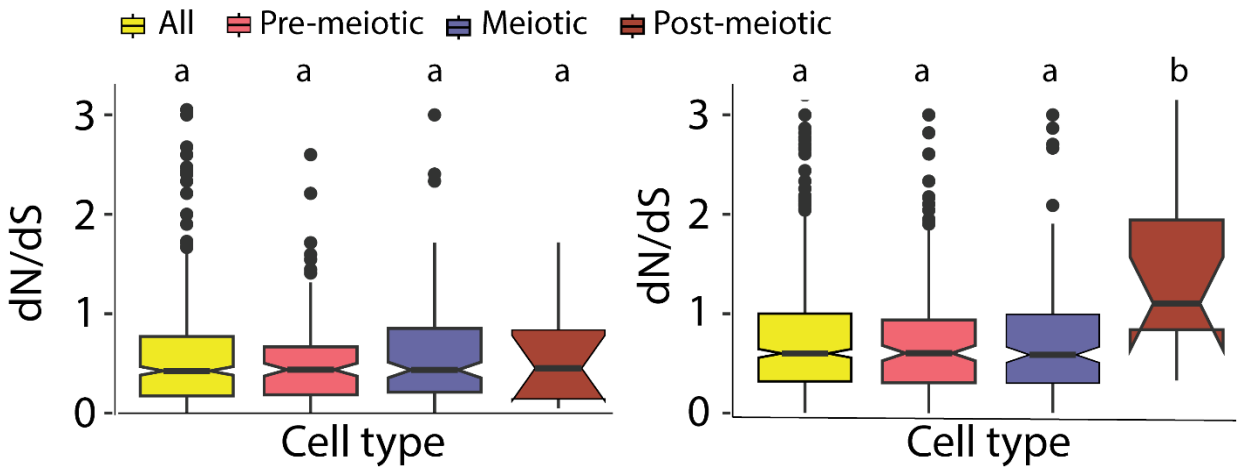

612

613

614 **Figure 5. Signatures of selection are largely the same across stages of spermatogenesis.**

615 Non-synonymous and synonymous substitutions were quantified between the threespine and

616 ninespine stickleback fish for X-linked and autosomal genes. There are no differences in d_N/d_S of

617 X-linked gametologs (left) across stages of spermatogenesis. d_N/d_S is similar across genes on

618 representative autosome 18 (right), except for an elevation in post-meiotic cell stages (Kruskal-

619 Wallis and Dunn's test, P = 0.006).

620

621

622 **Tables**

623 Table 1. Identification of clusters reveals genetic markers and gene ontology of distinct stages of
624 spermatogenesis.
625

Cluster identification	Characterization	Representative spermatogenic-related markers identified in cluster (P < 0.01)	Relevant GO terms (FDR < 0.01)
Early Spermatogonia	Undifferentiation, maintenance	*id4, npsn, ptpn6, myh9a, ctss2.1 hcls1, ponzr1, coro1a, itgb2, scinlb*	cell homeostasis, cell number homeostasis, NADP metabolic process
Late Spermatogonia	Differentiating, cell proliferation, hormones	*gata6, id1, ar, grnb, ptn, cyc1, prdx3, ctsa, h2ax*	Differentiation, chromosome, cell cycle
Early Spermatocytes	Early prophase, DSB formation	*smc2b, smc1al,hells, rab5c,rab35b,cbx3a, NASP,tex11*	core histone, centromere kinetochore, tubulin, ribosomal
Mid spermatocytes	Late prophase, DSB processing and strand invasion	*rad51, rad54, meig1, ccna1, map2k6,akirin2, cdk9, mns1, dyrk2, ccnb1*	embryo development, cell cycle, regulation of cell cycle, recombination
Mid-Late spermatocytes	Late meiosis, spindle assembly	*smc3, rab24, cenpv, cetn2,dnal1,cbx8b,rab8a,spag1,mospd1,cdc37*	chromosome organization, condensed chromosome, centromere, chromosome segregation, spindle

Late spermatocytes	Late meiosis, segregation and cell division	*cbx1, caprin1a, ccnb2, cfap57, SMARCA5, cdca8,rad23b, smc4,ncapd2,spata18,nu sap1, fzr1a*	Sister chromatid segregation, cell cycle, cilium organization, nuclear division, organelle fission, kinetochore
Early Spermatids	Spermiogenesis	*ak1, taf9, ybx1,map6a, dctn3*	Cilium, motile cilium, dynein complex, centriole
Late spermatid	Sperm maturation	*gapdh, gapdhs, krt18a.1, arpc3, myh9b*	Axoneme assembly, axoneme, ciliary plasm
Somatic cluster	Sertoli, erythrocytes, connective tissue, Leydig	*gata1a, hbae5, hbe1, ctrl, ccng1*	Myeloid cell homeostasis, erythrocyte development, immune system development

References

1. Ellis N, Goodfellow PN. The mammalian pseudoautosomal region. Trends Genet. 1989;5:406-10.
2. Turner JMA. Meiotic sex chromosome inactivation. Development. 2007;134(10):1823-31.
3. Turner JMA. Meiotic Silencing in Mammals. Annu Rev Genet. 2015;49(1):395-412.
4. Handel MA. The XY body: a specialized meiotic chromatin domain. Exp Cell Res. 2004;296(1):57-63.
5. Namekawa SH, Park PJ, Zhang L-F, Shima JE, McCarrey JR, Griswold MD, et al. Postmeiotic Sex Chromatin in the Male Germline of Mice. Curr Biol. 2006;16(7):660-7.
6. Turner JMA, Mahadevaiah SK, Ellis PJI, Mitchell MJ, Burgoyne PS. Pachytene Asynapsis Drives Meiotic Sex Chromosome Inactivation and Leads to Substantial Postmeiotic Repression in Spermatids. Dev Cell. 2006;10(4):521-9.
7. Shiu PK, Raju NB, Zickler D, Metzenberg RL. Meiotic silencing by unpaired DNA. Cell. 2001;107(7):905-16.

8. Turner JM, Mahadevaiah SK, Fernandez-Capetillo O, Nussenzweig A, Xu X, Deng CX, et al. Silencing of unsynapsed meiotic chromosomes in the mouse. Nat Genet. 2005;37(1):41-7.
9. Cortez D, Marin R, Toledo-Flores D, Froidevaux L, Liechti A, Waters PD, et al. Origins and functional evolution of Y chromosomes across mammals. Nature. 2014;508(7497):488-93.
10. Franco MJ, Sciurano RB, Solari AJ. Protein immunolocalization supports the presence of identical mechanisms of XY body formation in eutherians and marsupials. Chromosome Research. 2007;15(6):815-24.
11. Namekawa SH, Vandeberg JL, McCarrey JR, Lee JT. Sex chromosome silencing in the marsupial male germ line. Proceedings of the National Academy of Sciences. 2007;104(23):9730-5.
12. Daish TJ, Casey AE, Grutzner F. Lack of sex chromosome specific meiotic silencing in platypus reveals origin of MSCI in therian mammals. BMC Biol. 2015;13(1).
13. Murat F, Mbengue N, Winge SB, Trefzer T, Leushkin E, Sepp M, et al. The molecular evolution of spermatogenesis across mammals. Nature. 2023;613(7943):308-16.
14. Larson BJ, Van MV, Nakayama T, Engebrecht J. Plasticity in the Meiotic Epigenetic Landscape of Sex Chromosomes in Caenorhabditis Species. Genetics. 2016;203(4):1641-58.
15. Cabrero J, Teruel M, Carmona FD, Camacho JP. Histone H2AX phosphorylation is associated with most meiotic events in grasshopper. Cytogenet Genome Res. 2007;116(4):311-5.
16. Cabrero J, Teruel M, Carmona FD, Jiménez R, Camacho JP. Histone H3 lysine 9 acetylation pattern suggests that X and B chromosomes are silenced during entire male meiosis in a grasshopper. Cytogenet Genome Res. 2007;119(1-2):135-42.
17. Vibranovski MD, Lopes HF, Karr TL, Long M. Stage-Specific Expression Profiling of Drosophila Spermatogenesis Suggests that Meiotic Sex Chromosome Inactivation Drives Genomic Relocation of Testis-Expressed Genes. PLoS Genet. 2009;5(11):e1000731.
18. Vibranovski MD, Zhang YE, Kemkemer C, Lopes HF, Karr TL, Long M. Re-analysis of the larval testis data on meiotic sex chromosome inactivation revealed evidence for tissue-specific gene expression related to the drosophila X chromosome. BMC Biol. 2012;10(1):49.
19. Landeen EL, Muirhead CA, Wright L, Meiklejohn CD, Presgraves DC. Sex Chromosome-wide Transcriptional Suppression and Compensatory Cis-Regulatory Evolution Mediate Gene Expression in the Drosophila Male Germline. PLoS Biol. 2016;14(7):e1002499.
20. Kemkemer C, Hense W, Parsch J. Fine-Scale Analysis of X Chromosome Inactivation in the Male Germ Line of Drosophila melanogaster. Mol Biol Evol. 2011;28(5):1561-3.
21. Meiklejohn CD, Landeen EL, Cook JM, Kingan SB, Presgraves DC. Sex Chromosome-Specific Regulation in the Drosophila Male Germline But Little Evidence for Chromosomal Dosage Compensation or Meiotic Inactivation. PLoS Biol. 2011;9(8):e1001126.
22. Mikhaylova LM, Nurminsky DI. Lack of global meiotic sex chromosome inactivation, and paucity of tissue-specific gene expression on the Drosophila X chromosome. BMC Biol. 2011;9(1):29.
23. Betrán E, Thornton K, Long M. Retroposed new genes out of the X in Drosophila. Genome Res. 2002;12(12):1854-9.
24. Parisi M, Nuttall R, Naiman D, Bouffard G, Malley J, Andrews J, et al. Paucity of genes on the Drosophila X chromosome showing male-biased expression. Science. 2003;299(5607):697-700.
25. Wang PJ. X chromosomes, retrogenes and their role in male reproduction. Trends Endocrinol Metab. 2004;15(2):79-83.

26. Kruger AN, Brogley MA, Huizinga JL, Kidd JM, De Rooij DG, Hu Y-C, et al. A Neofunctionalized X-Linked Ampliconic Gene Family Is Essential for Male Fertility and Equal Sex Ratio in Mice. Curr Biol. 2019;29(21):3699-706.e5.
27. Mueller JL, Mahadevaiah SK, Park PJ, Warburton PE, Page DC, Turner JMA. The mouse X chromosome is enriched for multicopy testis genes showing postmeiotic expression. Nat Genet. 2008;40(6):794-9.
28. Soh YQ, Alföldi J, Pyntikova T, Laura, Graves T, Patrick, et al. Sequencing the Mouse Y Chromosome Reveals Convergent Gene Acquisition and Amplification on Both Sex Chromosomes. Cell. 2014;159(4):800-13.
29. Hughes JF, Skaletsky H, Pyntikova T, Koutseva N, Raudsepp T, Brown LG, et al. Sequence analysis in Bos taurus reveals pervasiveness of X–Y arms races in mammalian lineages. Genome Res. 2020;30(12):1716-26.
30. Bellott DW, Skaletsky H, Cho T-J, Brown L, Locke D, Chen N, et al. Avian W and mammalian Y chromosomes convergently retained dosage-sensitive regulators. Nat Genet. 2017;49(3):387-94.
31. Guioli S, Lovell-Badge R, Turner JMA. Error-Prone ZW Pairing and No Evidence for Meiotic Sex Chromosome Inactivation in the Chicken Germ Line. PLoS Genet. 2012;8(3):e1002560.
32. Federici F, Mulugeta E, Schoenmakers S, Wassenaar E, Hoogerbrugge JW, Van Der Heijden GW, et al. Incomplete meiotic sex chromosome inactivation in the domestic dog. BMC Genomics. 2015;16(1).
33. Wright AE, Darolti I, Bloch NI, Oostra V, Sandkam B, Buechel SD, et al. Convergent recombination suppression suggests role of sexual selection in guppy sex chromosome formation. Nature Communications. 2017;8(1):14251.
34. Darolti I, Wright AE, Mank JE. Guppy Y Chromosome Integrity Maintained by Incomplete Recombination Suppression. Genome Biology and Evolution. 2020;12(6):965-77.
35. Charlesworth D, Bergero R, Graham C, Gardner J, Keegan K. How did the guppy Y chromosome evolve? PLoS Genet. 2021;17(8):e1009704.
36. Lisachov AP, Zadesenets KS, Rubtsov NB, Borodin PM. Sex chromosome synapsis and recombination in male guppies. Zebrafish. 2015;12(2):174-80.
37. Peichel CL, McCann SR, Ross JA, Naftaly AFS, Urton JR, Cech JN, et al. Assembly of the threespine stickleback Y chromosome reveals convergent signatures of sex chromosome evolution. Genome Biology. 2020;21(1).
38. Roesti M, Moser D, Berner D. Recombination in the threespine stickleback genome—patterns and consequences. Mol Ecol. 2013;22(11):3014-27.
39. White MA, Kitano J, Peichel CL. Purifying Selection Maintains Dosage-Sensitive Genes during Degeneration of the Threespine Stickleback Y Chromosome. Mol Biol Evol. 2015;32(8):1981-95.
40. Ross JA, Peichel CL. Molecular cytogenetic evidence of rearrangements on the Y chromosome of the threespine stickleback fish. Genetics. 2008;179(4):2173-82.
41. Nath S, Welch LA, Flanagan MK, White MA. Meiotic pairing and double-strand break formation along the heteromorphic threespine stickleback sex chromosomes. Chromosome Research. 2022.
42. Lukassen S, Bosch E, Ekici AB, Winterpacht A. Single-cell RNA sequencing of adult mouse testes. Scientific Data. 2018;5(1):180192.

43. Craig-Bennett A. The Reproductive Cycle of the Three-Spined Stickleback, Gasterosteus aculeatus, Linn. Philosophical Transactions of the Royal Society of London Series B, Containing Papers of a Biological Character. 1931;219:197-279.
44. Heumos L, Schaar AC, Lance C, Litinetskaya A, Drost F, Zappia L, et al. Best practices for single-cell analysis across modalities. Nature Reviews Genetics. 2023;24(8):550-72.
45. Witt E, Benjamin S, Svetec N, Zhao L. Testis single-cell RNA-seq reveals the dynamics of de novo gene transcription and germline mutational bias in Drosophila. eLife. 2019;8.
46. Bonilla E, Xu EY. Identification and characterization of novel mammalian spermatogenic genes conserved from fly to human. Mol Human Reprod. 2008;14(3):137-42.
47. Lukassen S, Bosch E, Ekici AB, Winterpacht A. Characterization of germ cell differentiation in the male mouse through single-cell RNA sequencing. Scientific Reports. 2018;8(1).
48. Shami AN, Zheng X, Munyoki SK, Ma Q, Manske GL, Green CD, et al. Single-Cell RNA Sequencing of Human, Macaque, and Mouse Testes Uncovers Conserved and Divergent Features of Mammalian Spermatogenesis. Dev Cell. 2020;54(4):529-47.e12.
49. Green CD, Ma Q, Manske GL, Shami AN, Zheng X, Marini S, et al. A Comprehensive Roadmap of Murine Spermatogenesis Defined by Single-Cell RNA-Seq. Dev Cell. 2018;46(5):651-67.e10.
50. Hermann BP, Cheng K, Singh A, Roa-De La Cruz L, Mutoji KN, Chen IC, et al. The Mammalian Spermatogenesis Single-Cell Transcriptome, from Spermatogonial Stem Cells to Spermatids. Cell Reports. 2018;25(6):1650-67.e8.
51. Qian P, Kang J, Liu D, Xie G. Single Cell Transcriptome Sequencing of Zebrafish Testis Revealed Novel Spermatogenesis Marker Genes and Stronger Leydig-Germ Cell Paracrine Interactions. Frontiers in Genetics. 2022;13.
52. Wu X, Yang Y, Zhong C, Wang T, Deng Y, Huang H, et al. Single-Cell Atlas of Adult Testis in Protogynous Hermaphroditic Orange-Spotted Grouper, Epinephelus coioides. International Journal of Molecular Sciences. 2021;22(22):12607.
53. Lacerda SMdSN, Costa GMJ, de França LR. Biology and identity of fish spermatogonial stem cell. Gen Comp Endocrinol. 2014;207:56-65.
54. Xie X, Nóbrega R, Pšenička M. Spermatogonial Stem Cells in Fish: Characterization, Isolation, Enrichment, and Recent Advances of In Vitro Culture Systems. Biomolecules. 2020;10(4):644.
55. Hirota T, Blakeley P, Sangrithi MN, Mahadevaiah SK, Encheva V, Snijders AP, et al. SETDB1 Links the Meiotic DNA Damage Response to Sex Chromosome Silencing in Mice. Dev Cell. 2018;47(5):645-59.e6.
56. Sedelnikova OA, Pilch DR, Redon C, Bonner WM. Histone H2AX in DNA damage and repair. Cancer Biol Ther. 2003;2(3):233-5.
57. Cocquet J, Ellis PJI, Mahadevaiah SK, Affara NA, Vaiman D, Burgoyne PS. A Genetic Basis for a Postmeiotic X Versus Y Chromosome Intragenomic Conflict in the Mouse. PLoS Genet. 2012;8(9):e1002900.
58. Cocquet J, Ellis PJI, Yamauchi Y, Mahadevaiah SK, Affara NA, Ward MA, et al. The Multicopy Gene Sly Represses the Sex Chromosomes in the Male Mouse Germline after Meiosis. PLoS Biol. 2009;7(11):e1000244.
59. Moretti C, Blanco M, Ialy-Radio C, Serrentino ME, Gobé C, Friedman R, et al. Battle of the Sex Chromosomes: Competition between X and Y Chromosome-Encoded Proteins for

783 Partner Interaction and Chromatin Occupancy Drives Multicopy Gene Expression and Evolution
784 in Muroid Rodents. Mol Biol Evol. 2020;37(12):3453-68.
785 60. Bachtrog D, Mahajan S, Bracewell R. Massive gene amplification on a recently formed
786 Drosophila Y chromosome. Nature Ecology & Evolution. 2019;3(11):1587-97.
787 61. Hirano T. At the heart of the chromosome: SMC proteins in action. Nature Reviews
788 Molecular Cell Biology. 2006;7(5):311-22.
789 62. Moretti C, Vaiman D, Tores F, Cocquet J. Expression and epigenomic landscape of the
790 sex chromosomes in mouse post-meiotic male germ cells. Epigenetics & Chromatin.
791 2016;9(1).
792 63. Emerson JJ, Kaessmann H, Betrán E, Long M. Extensive Gene Traffic on the
793 Mammalian X Chromosome. Science. 2004;303(5657):537-40.
794 64. Shiao M-S, Khil P, Camerini-Otero RD, Shiroishi T, Moriwaki K, Yu H-T, et al. Origins
795 of New Male Germ-line Functions from X-Derived Autosomal Retrogenes in the Mouse. Mol
796 Biol Evol. 2007;24(10):2242-53.
797 65. Vibranovski MD, Zhang Y, Long M. General gene movement off the X chromosome in
798 the Drosophila genus. Genome Res. 2009;19(5):897-903.
799 66. Bell MA, Stewart JD, Park PJ. The World's Oldest Fossil Threespine Stickleback Fish.
800 Copeia. 2009;2009(2):256-65.
801 67. Ross JA, Urton JR, Boland J, Shapiro MD, Peichel CL. Turnover of Sex Chromosomes
802 in the Stickleback Fishes (Gasterosteidae). PLoS Genet. 2009;5(2):e1000391.
803 68. Varadharajan S, Rastas P, Löytynoja A, Matschiner M, Calboli FCF, Guo B, et al. A
804 high-quality assembly of the nine-spined stickleback (Pungitius pungitius) genome. Genome
805 Biology and Evolution. 2019.
806 69. Good JM, Nachman MW. Rates of protein evolution are positively correlated with
807 developmental timing of expression during mouse spermatogenesis. Mol Biol Evol.
808 2005;22(4):1044-52.
809 70. Kopania EEK, Larson EL, Callahan C, Keeble S, Good JM. Molecular Evolution across
810 Mouse Spermatogenesis. Mol Biol Evol. 2022;39(2).
811 71. Larson EL, Vanderpool D, Keeble S, Zhou M, Sarver BA, Smith AD, et al. Contrasting
812 Levels of Molecular Evolution on the Mouse X Chromosome. Genetics. 2016;203(4):1841-57.
813 72. Lifschytz E, Lindsley DL. The role of X-chromosome inactivation during
814 spermatogenesis. Proceedings of the National Academy of Sciences. 1972;69(1):182-6.
815 73. McKee BD, Handel MA. Sex chromosomes, recombination, and chromatin
816 conformation. Chromosoma. 1993;102(2):71-80.
817 74. Henking H. Über Patagonian pejerrey (Odontesthes hatcheri) spermatogenese und deren
818 Beziehung zur Entwicklung bei Pyrrhocoris apterus L. Zeitschrift für wissenschaftliche
819 Zoologie. 1891;51:685-736.
820 75. Solari AJ. The behavior of the XY pair in mammals. Int Rev Cytol. 1974;38(0):273-317.
821 76. Casey AE, Daish TJ, Barbero JL, Grützner F. Differential cohesin loading marks paired
822 and unpaired regions of platypus sex chromosomes at prophase I. Scientific Reports.
823 2017;7(1):4217.
824 77. Solari AJ. Equalization of Z and W axes in chicken and quail oocytes. Cytogenet Cell
825 Genet. 1992;59(1):52-6.
826 78. Schoenmakers S, Wassenaar E, Hoogerbrugge JW, Laven JSE, Grootegoed JA, Baarends
827 WM. Female Meiotic Sex Chromosome Inactivation in Chicken. PLoS Genet.
828 2009;5(5):e1000466.

79. Namekawa SH, Lee JT. XY and ZW: is meiotic sex chromosome inactivation the rule in evolution? PLoS Genet. 2009;5(5):e1000493.
80. Lisachov A, Dedukh D, Simanovsky S, Panthum T, Singchat W, Srikulnath K. Spaghetti Connections: Synaptonemal Complexes as a Tool to Explore Chromosome Structure, Evolution, and Meiotic Behavior in Fish. Cytogenet Genome Res. 2024;164(1):1-15.
81. Nanda I, Schories S, Simeonov I, Adolfi MC, Du K, Steinlein C, et al. Evolution of the Degenerated Y-Chromosome of the Swamp Guppy, Micropoecilia picta. Cells. 2022;11(7).
82. Meiklejohn CD, Tao Y. Genetic conflict and sex chromosome evolution. Trends in Ecology & Evolution. 2010;25(4):215-23.
83. Bachtrog D. The Y Chromosome as a Battleground for Intragenomic Conflict. Trends Genet. 2020;36(7):510-22.
84. Mank JE, Hosken DJ, Wedell N. Conflict on the sex chromosomes: cause, effect, and complexity. Cold Spring Harb Perspect Biol. 2014;6(12):a017715.
85. Good JM. The Conflict within and the Escalating War between the Sex Chromosomes. PLoS Genet. 2012;8(9):e1002955.
86. Lin Y, Darolti I, Furman BLS, Almeida P, Sandkam BA, Breden F, et al. Gene duplication to the Y chromosome in Trinidadian Guppies. Mol Ecol. 2022;31(6):1853-63.
87. Chang C-H, Gregory LE, Gordon KE, Meiklejohn CD, Larracuente AM. Unique structure and positive selection promote the rapid divergence of Drosophila Y chromosomes. eLife. 2022;11.
88. Mueller JL, Skaletsky H, Brown LG, Zaghlul S, Rock S, Graves T, et al. Independent specialization of the human and mouse X chromosomes for the male germ line. Nat Genet. 2013;45(9):1083-7.
89. Liu J, Shikano T, Leinonen T, Cano JM, Li M-H, Merilä J. Identification of Major and Minor QTL for Ecologically Important Morphological Traits in Three-Spined Sticklebacks (Gasterosteus aculeatus). G3 Genes|Genomes|Genetics. 2014;4(4):595-604.
90. Rollins JL, Chiang P, Waite JN, Von Hippel FA, Bell MA. Jacks and jills: Alternative life-history phenotypes and skewed sex ratio in anadromous threespine stickleback (Gasterosteus aculeatus). Evol Ecol Res. 2017;18(4):363-82.
91. Chang C-H, Mejia Natividad I, Malik HS. Expansion and loss of sperm nuclear basic protein genes in Drosophila correspond with genetic conflicts between sex chromosomes. eLife. 2023;12:e85249.
92. Larracuente AM, Presgraves DC. The selfish Segregation Distorter gene complex of Drosophila melanogaster. Genetics. 2012;192(1):33-53.
93. Ellis PJI, Bacon J, Affara NA. Association of Sly with sex-linked gene amplification during mouse evolution: a side effect of genomic conflict in spermatids? Hum Mol Genet. 2011;20(15):3010-21.
94. Olds-Clarke P. Models for male infertility: the t haplotypes. Rev Reprod. 1997;2(3):157-64.
95. Phadnis N, Orr HA. A Single Gene Causes Both Male Sterility and Segregation Distortion in Drosophila Hybrids. Science. 2009;323(5912):376-9.
96. Fitzpatrick JL. Sperm competition and fertilization mode in fishes. Philosophical Transactions of the Royal Society B: Biological Sciences. 2020;375(1813):20200074.
97. Verspoor RL, Price TAR, Wedell N. Selfish genetic elements and male fertility. Philos Trans R Soc Lond B Biol Sci. 2020;375(1813):20200067.

98. Van den Assem J. Territory in the three-spined stickleback Gasterosteus aculeatus L.: an experimental study in intra-specific competition: Brill Archive; 1967.
99. Largiadèr CR, Fries V, Bakker TCM. Genetic analysis of sneaking and egg-thievery in a natural population of the three-spined stickleback (Gasterosteus aculeatus L.). Heredity. 2001;86(4):459-68.
100. Nath S, Shaw DE, White MA. Improved contiguity of the threespine stickleback genome using long-read sequencing. G3 Genes|Genomes|Genetics. 2021;11(2).
101. Hao Y, Hao S, Andersen-Nissen E, Mauck WM, Zheng S, Butler A, et al. Integrated analysis of multimodal single-cell data. Cell. 2021;184(13):3573-87.e29.
102. Borg B. Effects of methyltestosterone on spermatogenesis and secondary sexual characters in the three-spined stickleback (Gasterosteus aculeatus L.). Gen Comp Endocrinol. 1981;44(2):177-80.
103. Sokołowska E, Kulczykowska E. Annual reproductive cycle in two free living populations of three-spined stickleback (Gasterosteus aculeatus L.): Patterns of ovarian and testicular development. Oceanologia. 2006;48.
104. Dapper AL, Payseur BA. Molecular evolution of the meiotic recombination pathway in mammals. Evolution. 2019;73(12):2368-89.
105. Ramesh MA, Malik S-B, Logsdon JM. A Phylogenomic Inventory of Meiotic Genes. Curr Biol. 2005;15(2):185-91.
106. Anders S, Pyl PT, Huber W. HTSeq--a Python framework to work with high-throughput sequencing data. Bioinformatics. 2015;31(2):166-9.
107. Wang D, Rastas P, Yi X, Löytynoja A, Kivikoski M, Feng X, et al. Improved assembly of the Pungitius pungitius reference genome. G3 Genes|Genomes|Genetics. 2024;14(8).
108. Slater GSC, Birney E. Automated generation of heuristics for biological sequence comparison. BMC Bioinformatics. 2005;6(1):31.
109. Cunningham F, Allen JE, Allen J, Alvarez-Jarreta J, Amode M R, Armean Irina M, et al. Ensembl 2022. Nucleic Acids Res. 2021;50(D1):D988-D95.
110. Yang Z. PAML 4: Phylogenetic Analysis by Maximum Likelihood. Mol Biol Evol. 2007;24(8):1586-91.
111. Blokhina YP, Nguyen AD, Draper BW, Burgess SM. The telomere bouquet is a hub where meiotic double-strand breaks, synapsis, and stable homolog juxtaposition are coordinated in the zebrafish, Danio rerio. PLoS Genet. 2019;15(1):e1007730.

Supplemental figures

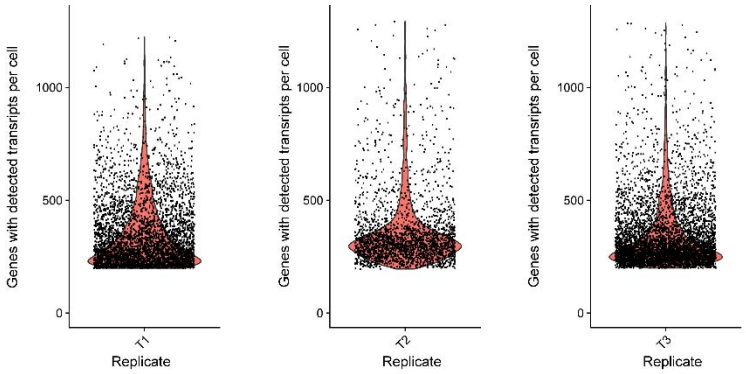

Supplemental Figure 1. Gene counts per samples.

Number of transcripts detected for each gene was totaled for each cell barcode within each of the three single cell RNA sequencing experiments. A similar distribution of detected genes were identified in each of three experiments.

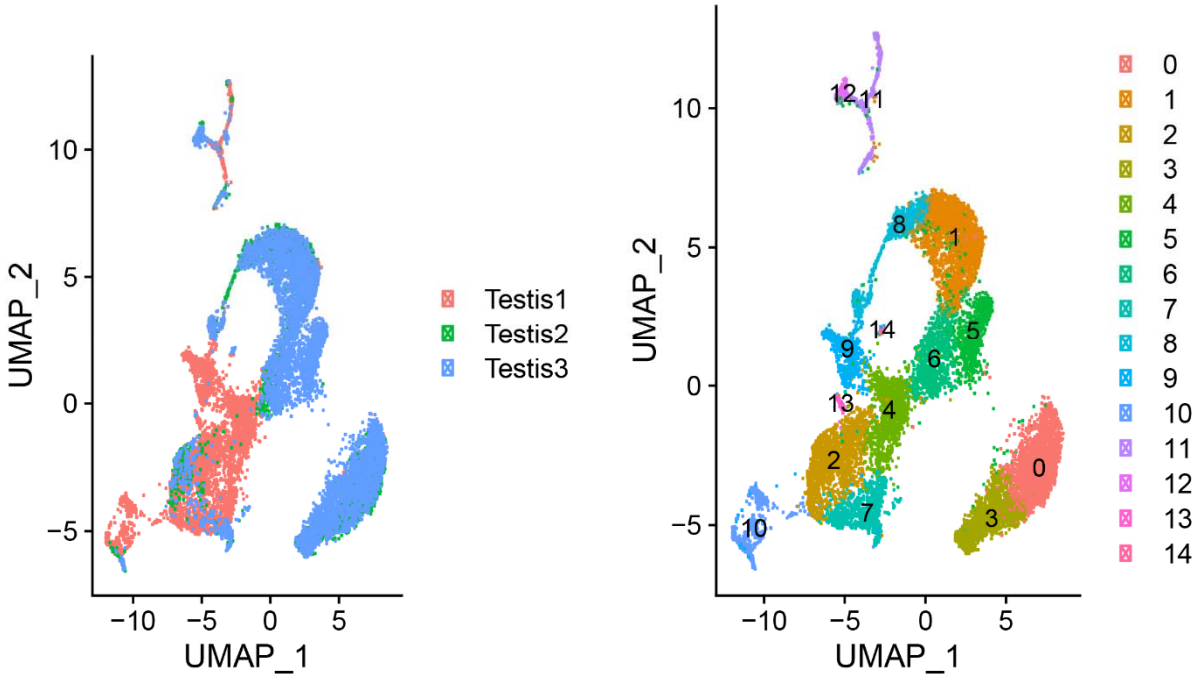

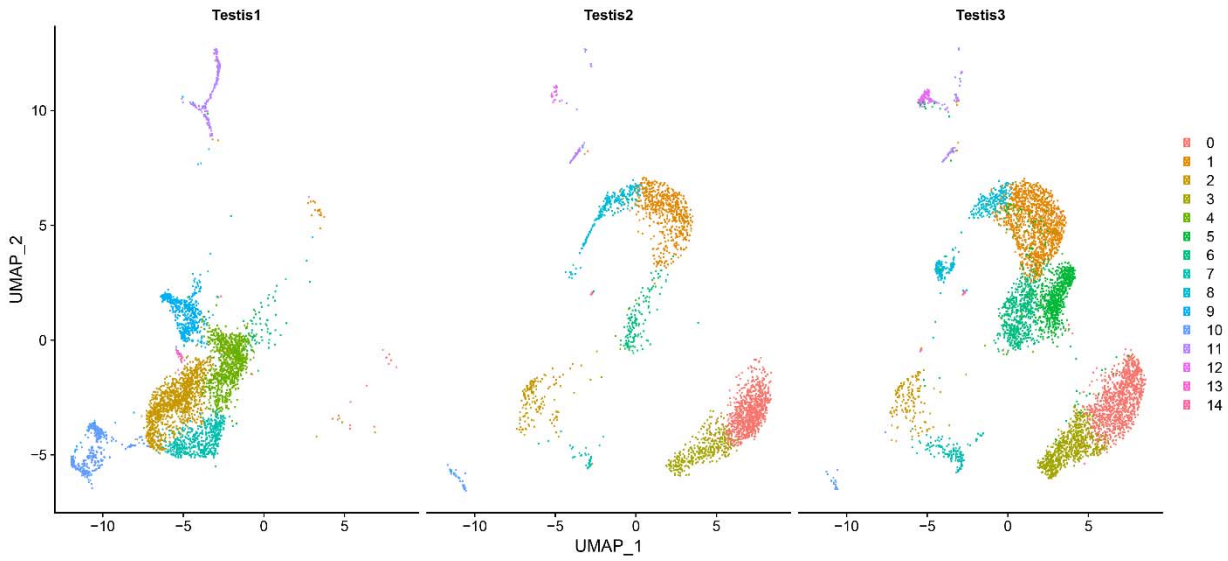

Supplemental Figure 2. Clusters split by sequencing replicate. Cell barcodes from all three sequencing runs were merged, and UMAP is depicted for all merged cells (top), and for each replicate separately (bottom). Proportion of each cell type within each sample was dependent on the onset of synchronous spermatogenesis in each individual. Only cell clusters identified in two of three replicates were used for downstream analysis.

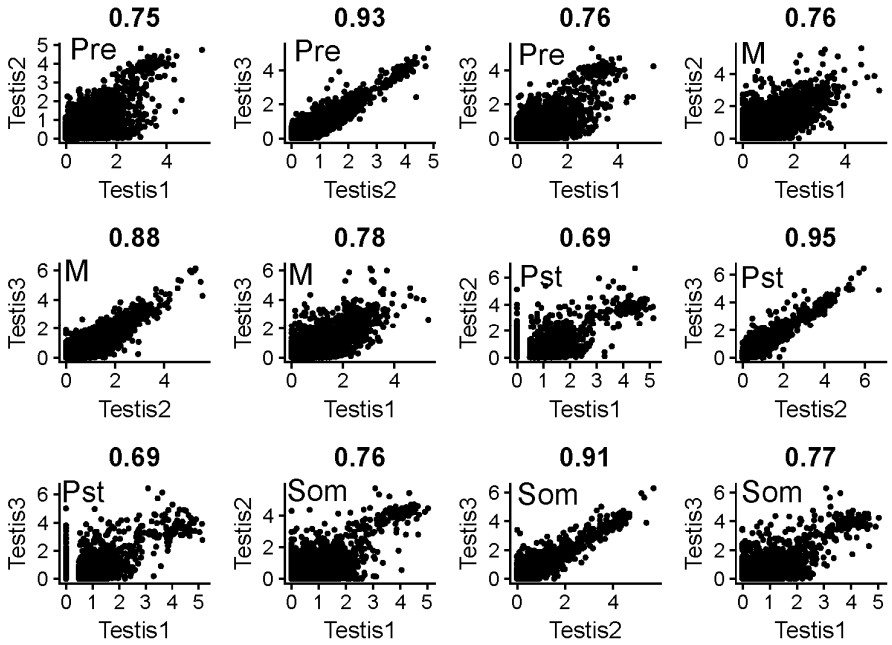

Supplemental Figure 3. Correlation of cluster expression profiles across replicates

Gene expression for all expressed genes identified in clusters were highly correlated (R > 0.69) across samples. Testis 2 and 3 showed stronger correlations across cell types compared to testis 1, likely due to a similar developmental staging at the time of testis dissociation. Spearman rank correlation is reported above each graph. Cell types are noted as Pre (pre-meiotic), M (meiotic), Pst (post-meiotic), and Som (somatic).

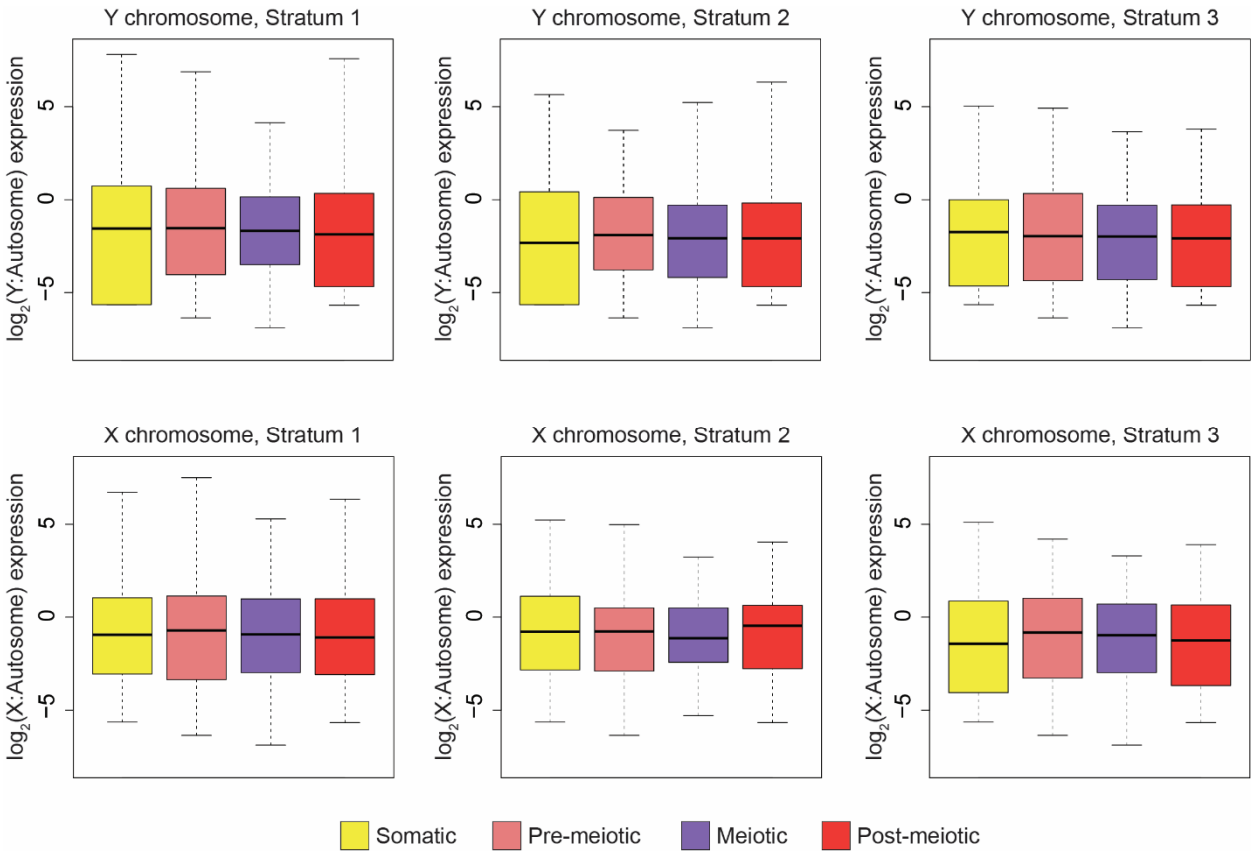

Supplemental Figure 4. Sex-linked gene expression across evolutonary strata.

Sex-linked gene expression does not change across spermatogenesis in the three different evolutionary strata. X- and Y-linked gene expression was normalized to median autosome

expression level for each stage of spermatogenesis. Relative to median autosome expression, X- (bottom) and Y-linked (top) gene expression does not change across stages of spermatogenesis across the three strata (stratum 1: oldest, stratum 2: middle, stratum 3: youngest). (Pairwise Mann-Whitney U Test, P > 0.05). Outliers are not shown.

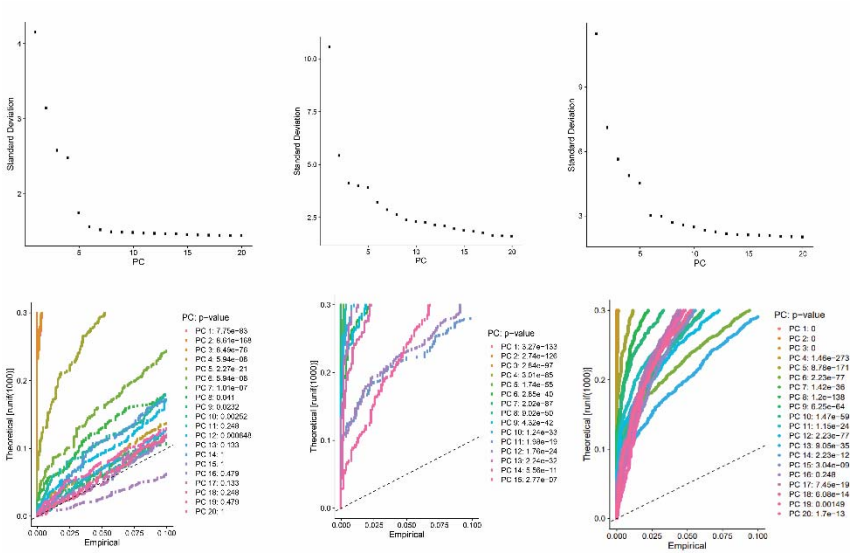

Supplemental Figure 5. Identification of significant principal components for scRNA-seq

Elbow plots and jackstraw simulations were generated to assess the number of significant principle components for each sequencing experiment.

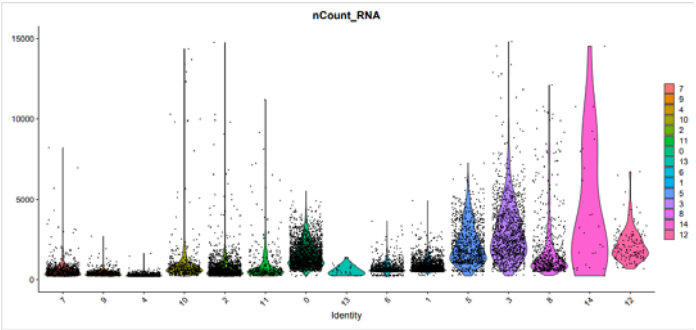

Supplemental Figure 6. Number of reads per cell type.

Number of RNA molecules identified per cell within each cell cluster were counted using Seurat.